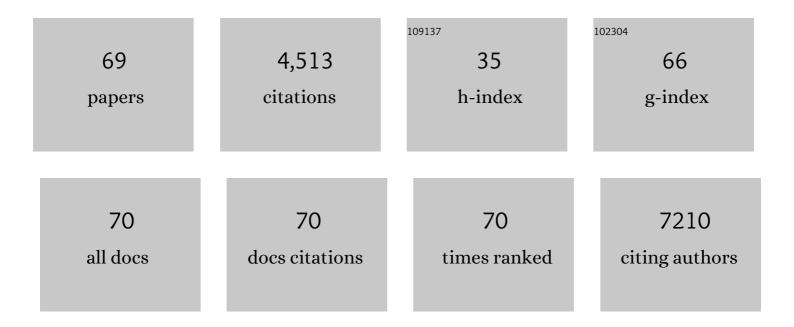
List of Publications by Year in descending order

Source: https://exaly.com/author-pdf/4882816/publications.pdf Version: 2024-02-01



ZHENHUA CHEN

#	Article	IF	CITATIONS
1	Incorporation of Graphenes in Nanostructured TiO ₂ Films <i>via</i> Molecular Grafting for Dye-Sensitized Solar Cell Application. ACS Nano, 2010, 4, 3482-3488.	7.3	471
2	Heterogeneous 2D/3D Tinâ€Halides Perovskite Solar Cells with Certified Conversion Efficiency Breaking 14%. Advanced Materials, 2021, 33, e2102055.	11.1	321
3	Vertically Aligned p-Type Single-Crystalline GaN Nanorod Arrays on n-Type Si for Heterojunction Photovoltaic Cells. Nano Letters, 2008, 8, 4191-4195.	4.5	298
4	ZnO/Au Composite Nanoarrays As Substrates for Surface-Enhanced Raman Scattering Detection. Journal of Physical Chemistry C, 2010, 114, 93-100.	1.5	190
5	Vertically Aligned ZnO Nanorod Arrays Sentisized with Gold Nanoparticles for Schottky Barrier Photovoltaic Cells. Journal of Physical Chemistry C, 2009, 113, 13433-13437.	1.5	174
6	Electrochemical doping of anatase TiO ₂ in organic electrolytes for high-performance supercapacitors and photocatalysts. Journal of Materials Chemistry A, 2014, 2, 229-236.	5.2	172
7	First lasing of an echo-enabled harmonic generation free-electron laser. Nature Photonics, 2012, 6, 360-363.	15.6	150
8	Surface Engineering of ZnO Nanostructures for Semiconductor‣ensitized Solar Cells. Advanced Materials, 2014, 26, 5337-5367.	11.1	149
9	Effect of Cerium Doping in the TiO ₂ Photoanode on the Electron Transport of Dye-Sensitized Solar Cells. Journal of Physical Chemistry C, 2012, 116, 19182-19190.	1.5	137
10	Quasiepitaxy Strategy for Efficient Fullâ€Inorganic Sb ₂ S ₃ Solar Cells. Advanced Functional Materials, 2019, 29, 1901720.	7.8	136
11	Highly anisotropic P3HT films with enhanced thermoelectric performance via organic small molecule epitaxy. NPG Asia Materials, 2016, 8, e292-e292.	3.8	131
12	Tuning Anionic Redox Activity and Reversibility for a High apacity Liâ€Rich Mnâ€Based Oxide Cathode via an Integrated Strategy. Advanced Functional Materials, 2019, 29, 1806706.	7.8	121
13	Synthesis, Characterization, and Photocatalytic Application of Different ZnO Nanostructures in Array Configurations. Crystal Growth and Design, 2009, 9, 3222-3227.	1.4	116
14	Large-Scale Synthesis and Phase Transformation of CuSe, CuInSe ₂ , and CuInSe ₂ /CuInS ₂ Core/Shell Nanowire Bundles. ACS Nano, 2010, 4, 1845-1850.	7.3	105
15	The effect of oxygen vacancy and spinel phase integration on both anionic and cationic redox in Li-rich cathode materials. Journal of Materials Chemistry A, 2020, 8, 7733-7745.	5.2	101
16	Hydrothermal synthesis of ordered single-crystalline rutile TiO2 nanorod arrays on different substrates. Applied Physics Letters, 2010, 96, .	1.5	97
17	High sensitivity of positive magnetoresistance in low magnetic field in perovskite oxide p–n junctions. Applied Physics Letters, 2005, 86, 032502.	1.5	92
18	High-Quality Graphenes via a Facile Quenching Method for Field-Effect Transistors. Nano Letters, 2009, 9, 1374-1377.	4.5	92

#	Article	IF	CITATIONS
19	Hybrid photovoltaic cells based on ZnO/Sb ₂ S ₃ /P3HT heterojunctions. Physica Status Solidi (B): Basic Research, 2012, 249, 627-633.	0.7	85
20	Improving the oxygen redox reversibility of Li-rich battery cathode materials via Coulombic repulsive interactions strategy. Nature Communications, 2022, 13, 1123.	5.8	81
21	Applications of silicon nanowires functionalized with palladium nanoparticles in hydrogen sensors. Nanotechnology, 2007, 18, 345502.	1.3	74
22	Tunable Electrical Properties of Silicon Nanowires via Surface-Ambient Chemistry. ACS Nano, 2010, 4, 3045-3052.	7.3	72
23	Template-Directed Bifunctional Dodecahedral CoP/CN@MoS ₂ Electrocatalyst for High Efficient Water Splitting. ACS Applied Materials & Interfaces, 2019, 11, 36649-36657.	4.0	70
24	Downward Homogenized Crystallization for Inverted Wideâ€Bandgap Mixedâ€Halide Perovskite Solar Cells with 21% Efficiency and Suppressed Photoâ€Induced Halide Segregation. Advanced Functional Materials, 2022, 32, .	7.8	63
25	Compositional optimization of a 2D–3D heterojunction interface for 22.6% efficient and stable planar perovskite solar cells. Journal of Materials Chemistry A, 2020, 8, 25831-25841.	5.2	59
26	Direct Growth of Graphene on Silicon by Metal-Free Chemical Vapor Deposition. Nano-Micro Letters, 2018, 10, 20.	14.4	57
27	Design of Low Crystallinity Spiro-Typed Hole Transporting Material for Planar Perovskite Solar Cells to Achieve 21.76% Efficiency. Chemistry of Materials, 2021, 33, 285-297.	3.2	57
28	A finely regulated quantum well structure in quasi-2D Ruddlesden–Popper perovskite solar cells with efficiency exceeding 20%. Energy and Environmental Science, 2022, 15, 296-310.	15.6	54
29	Controllable Synthesis of Vertically Aligned pâ€Type GaN Nanorod Arrays on nâ€Type Si Substrates for Heterojunction Diodes. Advanced Functional Materials, 2008, 18, 3515-3522.	7.8	50
30	Tunable p-Type Conductivity and Transport Properties of AlN Nanowires <i>via</i> Mg Doping. ACS Nano, 2011, 5, 3591-3598.	7.3	47
31	High-performance, fully transparent, and flexible zinc-doped indium oxide nanowire transistors. Applied Physics Letters, 2009, 94, .	1.5	46
32	Enhanced performance by incorporation of zinc oxide nanowire array for organic-inorganic hybrid solar cells. Applied Physics Letters, 2012, 100, .	1.5	43
33	Shape-controlled synthesis of organolead halide perovskite nanocrystals and their tunable optical absorption. Materials Research Express, 2014, 1, 015034.	0.8	43
34	MoC ultrafine nanoparticles confined in porous graphitic carbon as extremely stable anode materials for lithium- and sodium-ion batteries. Inorganic Chemistry Frontiers, 2017, 4, 289-295.	3.0	42
35	Modulating the molecular packing and distribution enables fullerene-free ternary organic solar cells with high efficiency and long shelf-life. Journal of Materials Chemistry A, 2019, 7, 20139-20150.	5.2	38
36	Surface ion transfer growth of ternary CdS1â^'xSex quantum dots and their electron transport modulation. Nanoscale, 2012, 4, 7690.	2.8	36

#	Article	IF	CITATIONS
37	Coherent nanoscale cobalt/cobalt oxide heterostructures embedded in porous carbon for the oxygen reduction reaction. RSC Advances, 2018, 8, 28625-28631.	1.7	32
38	Overcoming the carrier transport limitation in Ruddlesden–Popper perovskite films by using lamellar nickel oxide substrates. Journal of Materials Chemistry A, 2021, 9, 11741-11752.	5.2	28
39	Photoconductive Properties of Selenium Nanowire Photodetectors. Journal of Nanoscience and Nanotechnology, 2009, 9, 6292-6298.	0.9	26
40	Band alignment by ternary crystalline potential-tuning interlayer for efficient electron injection in quantum dot-sensitized solar cells. Journal of Materials Chemistry A, 2014, 2, 7004-7014.	5.2	26
41	ZnO nanowire arrays grown on Al:ZnO buffer layers and their enhanced electron field emission. Journal of Applied Physics, 2009, 106, .	1.1	24
42	Dye degradation induced by hydrogen-terminated silicon nanowires under ultrasonic agitations. Journal of Applied Physics, 2009, 105, 034307.	1.1	22
43	Self-catalytic Synthesis of ZnO Tetrapods, Nanotetraspikes, and Nanowires in Air at Atmospheric Pressure. Journal of Physical Chemistry C, 2008, 112, 9214-9218.	1.5	20
44	Stabilizing the Anionic Redox in 4.6 VÂLiCoO ₂ Cathode through Adjusting Oxygen Magnetic Moment. Advanced Functional Materials, 2022, 32, .	7.8	19
45	Suppressing Residual Lead Iodide and Defects in Sequentialâ€Deposited Perovskite Solar Cell via Bidentate Potassium Dichloroacetate Ligand. ChemSusChem, 2022, 15, .	3.6	18
46	First-principles study of single-walled armchair Cx(BN)y nanotubes. Solid State Communications, 2006, 137, 549-552.	0.9	17
47	Integrated Nanorods and Heterostructure Field Effect Transistors for Gas Sensing. Journal of Physical Chemistry C, 2010, 114, 7999-8004.	1.5	16
48	Energy band tunable TixSn1â^'xO2 photoanode for efficient non-TiO2 type dye sensitized solar cells. Journal of Materials Chemistry A, 2013, 1, 8453.	5.2	15
49	Tin Oxide Microspheres with Exposed {101} Facets for Dyeâ€sensitized Solar Cells: Enhanced Photocurrent and Photovoltage. ChemSusChem, 2014, 7, 172-178.	3.6	14
50	Delayed fluorescence material-assisted high performance ternary organic solar cells realized by prolonged exciton lifetime and diffusion length. Journal of Materials Chemistry C, 2020, 8, 17429-17439.	2.7	14
51	Epitaxial ZnS/Si core–shell nanowires and single-crystal silicon tube field-effect transistors. Journal of Crystal Growth, 2008, 310, 165-170.	0.7	13
52	Hysteresis in In2O3:Zn nanowire field-effect transistor and its application as a nonvolatile memory device. Applied Physics Letters, 2008, 93, 183111.	1.5	13
53	Solution-processable graphene oxide as an insulator layer for metal–insulator–semiconductor silicon solar cells. RSC Advances, 2013, 3, 17918.	1.7	13
54	Electronic structure at the interfaces of vertically aligned zinc oxide nanowires and sensitizing layers in photochemical solar cells. Journal Physics D: Applied Physics, 2011, 44, 325108.	1.3	12

#	Article	IF	CITATIONS
55	Substitution effects of Ru–terpyridyl complexes on photovoltaic and carrier transport properties in dye-sensitized solar cells. Journal of Materials Chemistry A, 2013, 1, 11033.	5.2	12
56	Inherited weak topological insulator signatures in the topological hourglass semimetal <mml:math xmlns:mml="http://www.w3.org/1998/Math/MathML"> <mml:mrow> <mml:msub> <mml:mi>Nb</mml:mi> <mml: <mml:math< td=""><td>mn>3<td>ıml:mn></td></td></mml:math<></mml: </mml:msub></mml:mrow></mml:math 	mn>3 <td>ıml:mn></td>	ıml:mn>

5